

## Original Article

# Inhibition of bone morphogenetic proteins signaling suppresses metastasis melanoma: a proteomics approach

Bhuvanesh Sukhlal Kalal<sup>1</sup>, Prashant Kumar Modi<sup>2</sup>, Dinesh Upadhy<sup>3</sup>, Pratip Saha<sup>4</sup>, Thottethodi Subrahmanya Keshava Prasad<sup>2</sup>, Vinitha Ramanath Pai<sup>1</sup>

<sup>1</sup>Department of Biochemistry, Yenepoya Medical College, Yenepoya (Deemed to be University), Mangaluru 575018, Karnataka, India; <sup>2</sup>Center for Systems Biology and Molecular Medicine, Yenepoya Research Centre, Yenepoya (Deemed to be University), Mangaluru 575018, Karnataka, India; <sup>3</sup>Centre for Molecular Neurosciences, Department of Anatomy, Kasturba Medical College, Manipal Academy of Higher Education Manipal, Udipi 576104, Karnataka, India; <sup>4</sup>Proteomics Facility, Thermo Fisher Scientific India Pvt Ltd, Bengaluru 560016, Karnataka, India

Received December 30, 2020; Accepted August 14, 2021; Epub October 15, 2021; Published October 30, 2021

**Abstract:** Background: Bone morphogenetic proteins (BMPs) are members of the transforming growth factor- $\beta$  superfamily, known to promote the tumor invasion and metastasis. There are continual progresses in understanding the role of BMP signaling pathways in carcinogenesis. However, the biological significance of BMPs in human melanoma has received very little attention. The study aimed to explore the effect of BMP inhibition on melanoma treated with LDN193189 (BMP inhibitor) using a quantitative proteomics approach in a melanoma xenograft model. Materials and methods: Melanoma tumor was induced in C57BL6 mice and treated intraperitoneally with LDN193189 for ten consecutive days. Post-treatment, tumors were collected, and comparative proteomics was performed using a high-resolution Orbitrap Fusion Tribrid mass spectrometer. Results: Treatment of melanoma with LDN193189 at 3 mg/kg body weight twice daily showed a significant decrease in the growth rate of the tumor compared to the other doses tested. Quantitative proteomic profiling identified 3231 proteins. Bioinformatics analysis of the 131 differentially expressed proteins selected by their relative abundance revealed that LDN193189 induces alterations in the cellular and metabolic process and the proteins that are involved in protein binding and catalytic activity in melanoma. Conclusions: Down-regulation of metallothionein (MT) 1 and MT2, emerging proteins for their role in tumor formation, progression, and drug resistance and transcription factor EB that plays a crucial role in the regulation of basic cellular processes, such as lysosomal biogenesis and autophagy, were identified upon inhibition of the BMP pathway in melanoma, suggesting their roles in melanoma growth. Understanding the role of these proteins will provide new directions for treating cancer.

**Keywords:** Chemotherapy, cancer, metallothionein, melanoma, proteomics, LDN193189, tumor

## Introduction

Melanoma is a highly aggressive skin cancer, which has the fastest and second-fastest-growing rate of cancer in men and women, respectively. Among all skin cancers, melanoma occurs only in 4% of cases but responsible for 80% of deaths [1]. The lifetime risk of melanoma is currently estimated to be 22.8 (100000), and is rising every year [2]. The unkindness of melanoma is that prognosis of an early diagnosed melanoma is good, but metastasized melanoma is incurable. Although it has the

fastest-growing incidence, the treatment efficiency of metastatic melanoma has not been significantly improved over the past 30 years, with a >10% survival rate in 5 years [3]. Surgery alone is clearly not beneficial to metastatic melanoma, and also melanoma is considered as a radio- and chemo-resistant tumor [4]. Although research is being done to treat melanoma with advanced knowledge of melanoma biology, the results are highly discouraging.

There are several combination chemotherapy regimens that are reported to have higher

response rates and are more effective for metastatic melanoma [5]. Currently, protein targeted therapies are being used to inhibit the growth of melanoma [6]. The most commonly used protein targeted therapy is EGFR pathway inhibition since melanoma is mostly driven by the mutations in EGFR, or its downstream molecules. However, recent studies showed that inhibition of EGFR pathway or its downstream molecules develops drug resistance [7]. Hence, inhibitors of other pathways are being tested for their effectiveness against the growth of melanoma.

Recent studies have shown that the bone morphogenetic protein (BMP) signaling cascade is dysregulated in malignant melanoma [8-10]. BMPs are members of the transforming growth factor- $\beta$  family. BMP has over 20 family members. Among them BMP-2, -4, -6, -7, and -9 are proposed as biomarkers for recurrence prediction and prognosis of cancer, and have been identified as novel prognostic biomarkers and potential therapeutic targets for cancer diagnosis and treatment [11]. BMP binds with cell surface receptor, serine/threonine kinase receptors (type I and type II) and form heteromeric complexes, thereby regulating the downstream signal transduction [12, 13].

BMPs activate various Smad dependent cascade as well as mitogen-activated protein kinase pathways [10]. They help in numerous cellular processes, such as proliferation, differentiation, motility, cell death, and are also linked to tumor formation and progression [11, 12]. Currently, there are several FDA-approved drugs available to target the BMP receptors. LDN-193189 is a small molecule inhibitor of BMP type I receptors and multi-kinase inhibitors that can target the kinases of BMP, MAPK14 (p38), MAPK8 (JNK), AKT, and mTOR signaling experimental models [14, 15].

Mouse models are essential in cancer research and useful to study the tumor development and cancer progression by histopathology, genetic profiles, and response to therapeutics. The present study shows that inhibition of BMP pathway is a potential target for treating metastatic melanoma. However, further evidence is required to confirm the results. The present study compared melanoma proteomes of mouse models based on quantitative mass spectrometry.

### Materials and method

#### *Cell lines and cell culture*

Mouse melanoma cell line B16F10 was purchased from the National Centre for Cell Science (Pune, India). Cells were grown in Dulbecco's Modified Eagle Medium (Himedia, India) supplemented with 2 mM L-glutamine, 10% fetal bovine serum (Himedia, India), and 1% antibiotics (100 U/mL penicillin G and 100 mg/mL streptomycin) (Himedia, India), and maintained at 37°C in a humidified incubator of 5% CO<sub>2</sub>. BMP inhibitor (LDN193189) was purchased from Sigma-Aldrich (St. Louis, MO, USA) and dissolved in dimethyl sulfoxide (DMSO) (Himedia, India) and stored at -20°C as aliquots, for single-time use.

#### *Measurement of cell viability*

Cell viability was measured by 3-(4,5-Dimethylthiazol-2-yl)-2,5-Diphenyltetrazolium Bromide (MTT) assay using the methods published earlier [16]. Cells were treated with different concentrations of LDN193189 or vehicle (DMSO) for 72 h as described earlier [17, 18], and the 50% inhibition concentrations (IC<sub>50</sub>) were derived from the dose-response curve.

#### *Animals and care*

Institutional Animal Ethical Committee approval (Reference no. 2014/1702) was taken prior to animal study. Committee for the Purpose of Control and Supervision of Experiments on Animals (CPCSEA) guidelines were strictly followed for the animal treatment.

Pathogen-free C57BL/6 mice, 6-8 weeks of age, both male and female, weighing 25±5 g were selected for the study from an inbred colony. All the animals were housed in a sterile polypropylene cage containing sterile paddy husk as bedding material and maintained under controlled conditions of temperature (23±2°C), humidity (55±5%) and light/dark (12 hour each) with sterile food and water *ad libitum*.

#### *Melanoma induction in mice*

The C57BL/6 mice were injected with a subcutaneous flank injection of B16F10 cells (5 × 10<sup>5</sup>) suspended in phosphate buffered saline (100  $\mu$ L). The animals were checked every day

## Effectiveness of BMP inhibition on melanoma

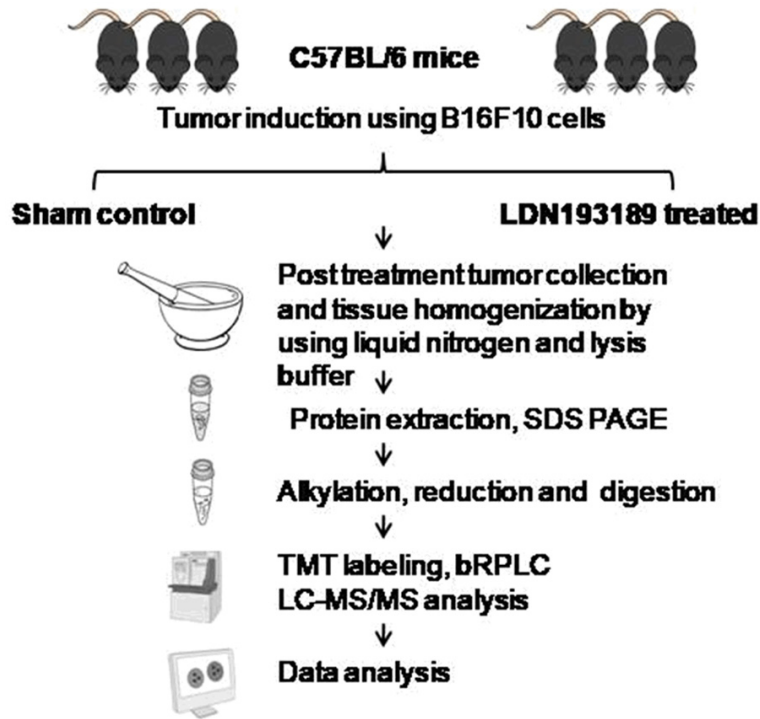


**Figure 1.** Flowchart of LC-MS/MS for a comparative analysis of protein expression in LDN193189 treated melanoma.

for signs of a tumor and once visualized, tumor size was measured using vernier caliper and tumor volume was calculated by the formula: volume (mm<sup>3</sup>) = (0.52) × (length) × (width) × (height) (in mm). When the tumor attained a diameter of 100 mm, it was used for the drug treatment.

### LDN-193189 treatment

Sham controls were injected with PBS (100 µL). Tumor-bearing mice were divided into different groups and treated intraperitoneally with LDN193189 using 1 cc syringe for 10 consecutive days.

### Treatment groups

Group 1. Sham control.

Group 2. Two mg/kg body weight, intraperitoneal injection, twice a day.

Group 3. Three mg/kg body weight, intraperitoneal injection, once a day.

Group 4. Three mg/kg body weight, intraperitoneal injection, twice a day.

### Procurement of specimens

For proteomic profiling of melanoma, sham-treated group and treatment group (with BMP inhibitor LDN-193189 at a dose of 3 mg/kg body weight, intraperitoneally injected, every 12 h, for ten consecutive days) were selected. Upon completion of the treatment, animals were sacrificed by cervical dislocation, the tumors were harvested (from both sham control and treatment groups) and snap frozen in liquid nitrogen and kept at -80°C until further use.

### Mass spectrometric analysis

The proteomic analysis was done by liquid chromatography with tandem mass spectrometry (LC-MS-MS) and four tumors from each control and treatment were used (**Figure 1**).

**Sample preparation:** The samples were snap-frozen in liquid nitrogen and lysed with lysis buffer containing 50 mM triethylammonium bicarbonate (TEABC), 4% sodium dodecyl sulfate (SDS) and phosphatase inhibitor (1 mM sodium orthovanadate, 2.5 mM sodium pyrophosphate and 1 mM β-glycerophosphate) and sonicated. The samples were heated at 95°C for 5 min, cooled to room temperature, and centrifuged at 12,000 rpm for 15 min at 4°C and the supernatant was collected. Protein estimation was performed using bicinchoninic acid (BCA) protein assay kit (Thermo Scientific, Massachusetts, USA).

**Alkylation, reduction, and trypsin digestion:** In-solution digestion was carried out as previously described [19]. Briefly, 300 µg protein from each condition was taken and reduced with 10 mM DTT at 60°C for 20 min and alkylated with 20 mM IAA at room temperature for 10 min in the dark. Acetone precipitation of protein was carried out by using six volumes of acetone and incubated at -20°C for 12 h, and protein was pelleted by centrifugation at 13,000 rpm for 20 min at 4°C. The pellet was resuspended in 50 mM TEABC and then digest-

## Effectiveness of BMP inhibition on melanoma

ed with trypsin (1:20; trypsin:protein; Worthington) at 37°C, overnight. The peptides were dried using SpeedVac (Thermo Scientific) and used for TMT labeling dissolved in bRPLC solution A (1 mL; pH 9), centrifuged (16,000 × g for 5 min at 4°C), and the supernatant transferred to fresh microfuge tubes. Fractionation of the peptide digest was done using basic reverse phase chromatography. Each fraction (10%) was separated for liquid chromatography-tandem mass spectrometry (LC-MS/MS) analysis of the total proteome.

**TMT labeling:** Three hundred micrograms of trypsin-digested peptides from each group was labeled with Amine-Reactive Tandem Mass Tag Reagents (TMT6 Label Reagents; Thermo Scientific; #90068) according to the manufacturer's protocol. The TMT labels were reconstituted before labeling in 41 µL of anhydrous acetonitrile (Sigma Aldrich) and added to the appropriate sample for labeling over 1 h at room temperature (RT). The tumor from sham control group was labeled with reagent 126, 127 and 128, and the treatment group was labeled with 129, 130 and 131. After 15 minutes, 8 µL of 5% hydroxylamine was added to quench each reaction. After quenching the reaction all samples were pooled together and processed for fractionation by bRPLC.

**Basic reverse-phase LC-based fractionation (bRPLC):** Fractionation of the TMT labeled pooled peptide digest was done using basic reverse phase chromatography. The pooled digested sample was loaded on Waters XBridge column (Waters Corporation, Milford, MA, USA; 130Å, 5 µm, 250 × 4.6 mm) using a Hitachi LaChrom Elite HPLC system, maintaining a flow rate of 0.5 mL/min. The peptide separation was achieved using a 130-min gradient at a flow rate of 0.5 mL/min of solvent A (10 mM TEABC buffer, pH ~8.5) and B (10 mM TEABC buffer, 90% acetonitrile, pH ~8.5). The fractionation was continued at 97% solvent A for 20 min, followed by 3% solvent B for 0-5 min, 10% solvent B for 5-10 min, 10-35% solvent B for 10-40 min, and 100% solvent B for 40-45 min gradient. Flow-through fractions were collected in a 96-well plate and were finally concatenated into six fractions. Pooled fractions were lyophilized and stored at -80°C until they were subjected to tandem MS analysis.

**LC-MS/MS analysis:** LC-MS/MS analysis of the samples was performed using Q-Exactive plus hybrid quadrupole-Orbitrap mass spec-

rometer (Thermo Fisher Scientific, Bremen, Germany) interfaced with Easy-nLC-1200 (Thermo Scientific, Bremen, Germany). The peptides obtained after C18 cleaning were resuspended in 0.1% formic acid (Solvent A) and loaded onto the trap column (Thermo Scientific, 75 µm × 2 cm, nanoViper, 3 µm, 100 Å) filled with C18 at a flow rate of 4 µL/min. The peptides were further resolved onto an analytical column (Thermo Scientific EASY-Spray RSLC C18 2 µm 15 × 50 µm) with a flow rate of 300 nL/min, using a step gradient of 5-35% solvent B (0.1% formic acid in 80% acetonitrile) for first 105 min and 35-100% solvent B for 105-126 min. The total run time was set to 130 min. Data were acquired in data-dependent acquisition mode at a scan range of 400-1600, and in positive mode with a maximum injection time of 55 msec using an Orbitrap mass analyzer at a mass resolution of 70,000 at 400 m/z. Top 15 intense precursor ions were selected for each duty cycle and subjected to higher energy collision-induced dissociation with 34% normalized collision energy.

### *Bioinformatics data analysis*

MS-derived data were analyzed with Proteome Discoverer software, version 2.1 (Thermo Scientific) with the SEQUEST HT and Mascot (version 2.5.1; Matrix Science, London, United Kingdom) search algorithms. It was searched against Mouse RefSeq 83 protein database (containing 76,332 entries with common contaminants). The common nodes for PD search include spectrum selector, MASCOT, SEQUEST search nodes, peptide validator, event detector, and precursor quantifier. Oxidation of methionine was set as a fixed modification. TMT labeling at lysine and carbamidomethylation of cysteine were set as variable modifications. The precursor mass tolerance was set at 10 ppm, and 0.05 Da was set for fragment ion tolerance. Trypsin was used as a proteolytic enzyme with a maximum of two missed cleavages. The data were searched against the decoy database with a 1% false discovery rate cutoff at the peptide level. The abundance information of proteins was extracted from PD into excel files. The intensity values of the proteins in the datasheet were normalized, and fold changes in treated tissue versus control tissue were calculated. The cutoff values of different proteins were appointed as follows: a relative abundance of more than 1.5 times was considered up-regulated or lower than 0.66

## Effectiveness of BMP inhibition on melanoma

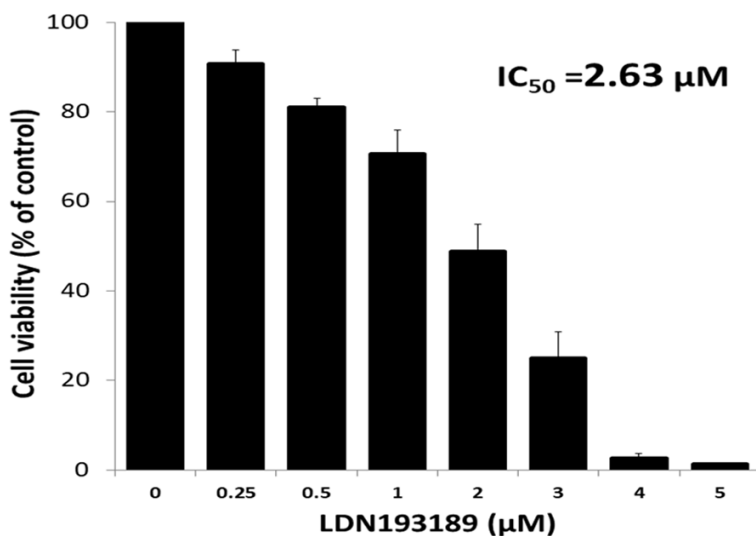


**Figure 2.** Cytotoxic effect of LDN193189 against mouse melanoma cells (B16F10). For MTT assay, B16F10 cells were treated with LDN193189 (0.25–5 µM) for 72 h. Data shown are mean  $\pm$  SD of three replicate wells. A graph was plotted with concentration of LDN193189 (X-axis) vs. cell viability % (Y-axis) and the  $IC_{50}$  values were calculated using the formula  $y=b+ax$ . An  $IC_{50}$  value is the concentration of the drug which results in 50% cell death.

times as down-regulated. Further biological network analysis was performed using several bioinformatics tools with the *Mus musculus* genome as a background dataset such as DAVID Pathway analysis tool [20], Panther Pathway analysis tool [21], Human Protein Reference Database (HPRD) [22], and String Protein interaction analysis [23].

**Availability of data:** The mass spectrometry-derived data generated in this study were deposited to the ProteomeXchange Consortium [24] via the PRIDE partner repository with the dataset identifier PXD016088.

**Statistical analysis:** The data are presented as mean  $\pm$  standard deviation (mean  $\pm$  SD), and the significance between groups was analyzed by one-way analysis of variance (one-way ANOVA). The statistical significance was determined with a *P*-value threshold of  $<0.05$ . All experiments were repeated more than three times. Statistical analysis was performed using SPSS version 20 (SPSS, Inc., Chicago, IL, USA).

### Results

#### Estimation of $IC_{50}$ of LDN193189

MTT assay showed that after treatment with varying concentrations of LDN193189, there

was a concentration-dependent reduction in cell viability. The  $IC_{50}$  values were 2.63 µM in B16F10 (Figure 2).

#### Quantification of LDN193189 dose for animal study

Three different doses of LDN193189 were used to assess the effective antitumor dose of LDN193189 and compared with the control group. The tumor of the control group showed continual growth. While the treatment of melanoma with 2 mg/kg body weight twice daily and 3 mg/kg body weight once daily delayed the tumor growth as compared to tumors in control group (Figure 3).

However, treatment of melanoma with LDN193189 at 3 mg/kg body weight twice daily showed a significant decrease in the rate of growth of the tumor as compared to the other doses tested. At this dose, the mice did not show any impairment of motion. In addition, postmortem examination of organs such as heart, liver, lungs, kidneys, and spleen, did not show any changes in the size. The visual examination of melanoma tumors showed complete necrosis of tissues (Figure 4).

#### Identification of differentially expressed proteins by tandem mass spectrometry

For proteomic analysis, three biological replicates of control tumor and treatment tumor (3 mg/kg body weight, twice daily) were used. All six fractions of mouse melanoma tissue were analyzed for total proteome. The data obtained for LC-MS/MS were searched against the mouse reference database using Proteome discoverer 2.1, which identified 3231 proteins. The proteins within a group are ranked according to the number of peptides, the number of PSMs, their protein scores, and the sequence coverage. Of the 3231 proteins, 117 were up-regulated (fold change  $\geq 1.5$ ) while 14 were down-regulated (fold change  $\leq 0.66$ ).

This study performed global proteomic profiling of the mouse melanoma tissue treated with

## Effectiveness of BMP inhibition on melanoma

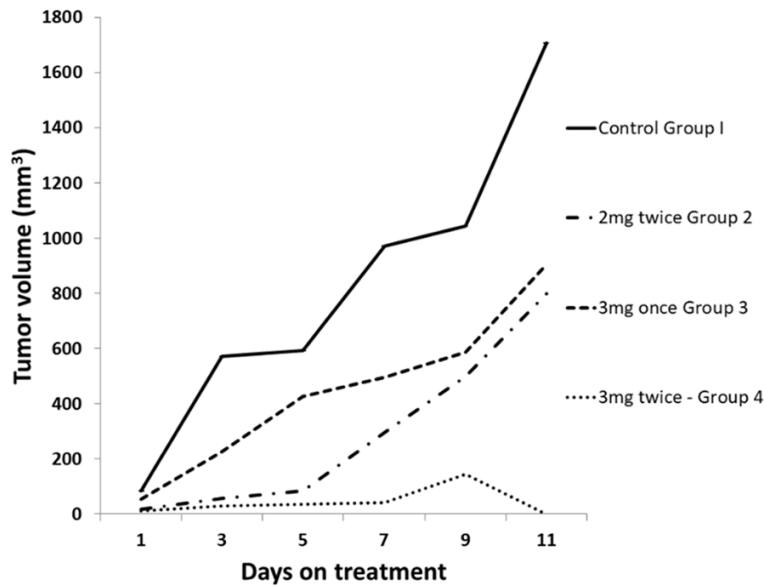


**Figure 3.** Effect of varying doses of LDN193189 on tumor growth in C57BL/6 mice. Mice were injected with B16F10 cells ( $2 \times 10^5$ ) suspended in phosphate buffered saline (100  $\mu$ L). Once the tumor reached a size of 100 mm<sup>3</sup>, control group was injected with normal saline, while treatment group was injected with BMP inhibitor LDN-193189 at different doses for 10 consecutive days (x-axis days 1 to 10). The values plotted are a mean of 3 animals in each group.

LDN193189 (BMP inhibitor) using in-solution methods. bRPLC fractionation yielded six fractions, which were subjected to LC-MS/MS analysis. Analysis of the LC-MS/MS data led to the identification of a total of 3231 nonredundant proteins. A schematic representation of the workflow employed for the analysis using a Q-Exactive plus hybrid quadrupole-Orbitrap mass spectrometer is shown in **Figure 1**. The complete list of the identified proteins is provided in the [Supplementary Table 1](#) and a partial list of top 10 upregulated, and 10 most downregulated proteins are given in **Table 1**.

### *Functional classification of proteins altered after LDN193189 treatment in melanoma tissue*

Proteins orchestrate various biochemical pathways and are involved in structural and functional aspects of cells and tissues. To better understand the functionality of the altered proteins identified after LDN193189 treatment, we carried out functional annotation using PANTHER to classify proteins based on their biological processes, molecular functions, and subcellular localization (**Figure 5**). Molecular functions showed majority of the proteins involved in protein binding (40.7%) and catalyt-

ic activity (36.1%). The sub-cellular localization analysis showed that a majority of the proteins are intracellular (43.8%) and in cell organelles (23.5%). The analysis of the biological process revealed a maximal number of proteins to be involved in cellular process (34.7%) and metabolic process (24.6%).

Pathway enrichment analysis showed that most of the identified proteins are involved in complement and coagulation cascades, platelet activation, and regulation of actin cytoskeleton (**Figure 6**). String analysis showed that the protein involved in cell components and biological processes are those with most common interactions (**Figure 7**). Representative spectra of the proteins identified in our study are provided in **Figure 8**.

## Discussion

Malignant melanoma is one of the most aggressive human neoplasms and its incidence is still increasing. The BMP signaling plays dual role of development and invasion event in cancer by affecting, at the cellular and molecular levels, epithelial mesenchyme transition, cancer stem cells and angiogenesis [25]. BMP has been shown to regulate multiple downstream pathways including PI3K/AKT, MAPK/ERK, NF- $\kappa$ B, and STAT3 pathways, and SMAD signaling pathways [12]. Therefore BMP pathway is an attractive target for blocking the tumor growth.

LDN193189 is a selective inhibitor of BMP signaling for the BMP type I receptors, activin receptor-like kinase 1 (ALK1), ALK2, and ALK3. It can block cell migration and increase survival by reducing the proliferation and increasing apoptosis of cancer cells [26-28]. LDN193189 blocks the activation of Smad and non-Smad pathways by modulating MAPKs p38, ERK1/2 and the Akt pathway [13, 29]. LDN193189 was also reported to inhibit the growth of breast and prostate cancers *in vivo* and prolong survival of mice bearing ovarian cancer cells which demonstrated that LDN193189 reduced the

## Effectiveness of BMP inhibition on melanoma



**Figure 4.** B16F10 melanoma tumor at day 1 and day 7 in control untreated group and treated group. Mice were injected with  $5 \times 10^5$  B16F10 cells suspended in 100  $\mu$ L phosphate buffered saline. Once the tumor reached a size of 100 mm<sup>3</sup>, Control group was injected with normal saline while treatment group was injected with BMP inhibitor LDN193189 at a dose of 3 mg/kg body weight twice daily for ten consecutive days.

**Table 1.** Genes and the fold change of proteins altered in the LDN193189 treated melanoma tissue

Sl no	Up-regulated (fold change $\geq 1.5$ )			Down-regulated (fold change $\leq 0.66$ )		
	Gene Symbol	Description	Fold change	Gene Symbol	Description	Fold change
1	Car2	carbonic anhydrase 2 isoform X1	7.813	Mt2	metallothionein-2	0.266
2	Hbb-bt	hemoglobin, beta adult t chain	6.061	Ccdc126	coiled-coil domain-containing protein 126 isoform 1 precursor	0.276
3	Pvalb	parvalbumin alpha isoform X1	4.565	Mt1	metallothionein-1	0.286
4	Hba-a2	hemoglobin alpha, adult chain 2	4.242	Yaf2	YY1-associated factor 2 isoform X1	0.334
5	Scrn3	secernin-3 isoform X1	3.952	Tfeb	transcription factor EB isoform a	0.355
6	Slc4a1	band 3 anion transport protein	3.933	Serpina1e	alpha-1-antitrypsin 1-5 precursor	0.361
7	Fga	fibrinogen alpha chain isoform 1 preproprotein	3.582	Hist2h2aa2	histone H2A type 2-A	0.477
8	Fgg	fibrinogen gamma chain isoform 2 precursor	3.427	Hacd2	3-Hydroxyacyl-CoA Dehydratase 2	0.477
9	Fgb	fibrinogen beta chain preproprotein	3.360	Hspb1	heat shock protein beta-1	0.485
10	Tnnc2	troponin C, skeletal muscle	3.155	Hmga1	high mobility group protein HMG-I/HMG-Y isoform a	0.527

The data shown in the table are the altered proteins in the LDN193189 treated as compared to the untreated controls. The data obtained for LC-MS/MS were analyzed using Proteome discoverer 2.1, which compares the LC-MS/MS data against mouse database. This table shows 10 proteins with highest fold increase and 10 proteins which are most down-regulated, their gene symbol, and their fold change, i.e., concentration in LDN193189 treated melanoma/concentration in untreated melanoma.

viability and enhanced the chemosensitivity of Smad4-silenced CRC cells *in vitro*. However, LDN193189 treatment has shown to enhance the metastatic property of bone [27]. In the present study, we used LDN193189 to demonstrate its anticancer activity for melanoma tumor.

LDN193189 has greater potency than its structural analog dorsomorphin and even low concentration (0.5  $\mu$ M) is sufficient to inhibit phosphorylation of BMP mediated Smad activation [30]. In the present study we treated the mouse model with a dose of 3 mg/kg every 12 h, which has already been used in several earlier studies [26, 27, 30, 31]. Administration of the LDN193189 (3 mg/kg intraperitoneally every 12 h) was able to inhibit tumor growth

and visual examination showed complete necrosis of the tumor. This may be because LDN193189 was able to inhibit activation of SMAD1/5/8 and the downstream transcriptional activity which is induced by ALK2 in affected tissues [30]. In mice, the dose of 3 mg/kg every 12 h of LDN193189 showed no impairment of motion and no damage to vital organs such as the heart, liver, lungs, kidneys, and spleen, suggesting that it is a safe dose.

Quantitative proteomics is an emerging tool for identifying active and alteration in molecular pathways to understand the pathogenesis mechanisms, drug action, and resistance of diseases [32]. The present study compared melanoma proteomes of mouse models on the basis of quantitative mass spectrometry.

## Effectiveness of BMP inhibition on melanoma

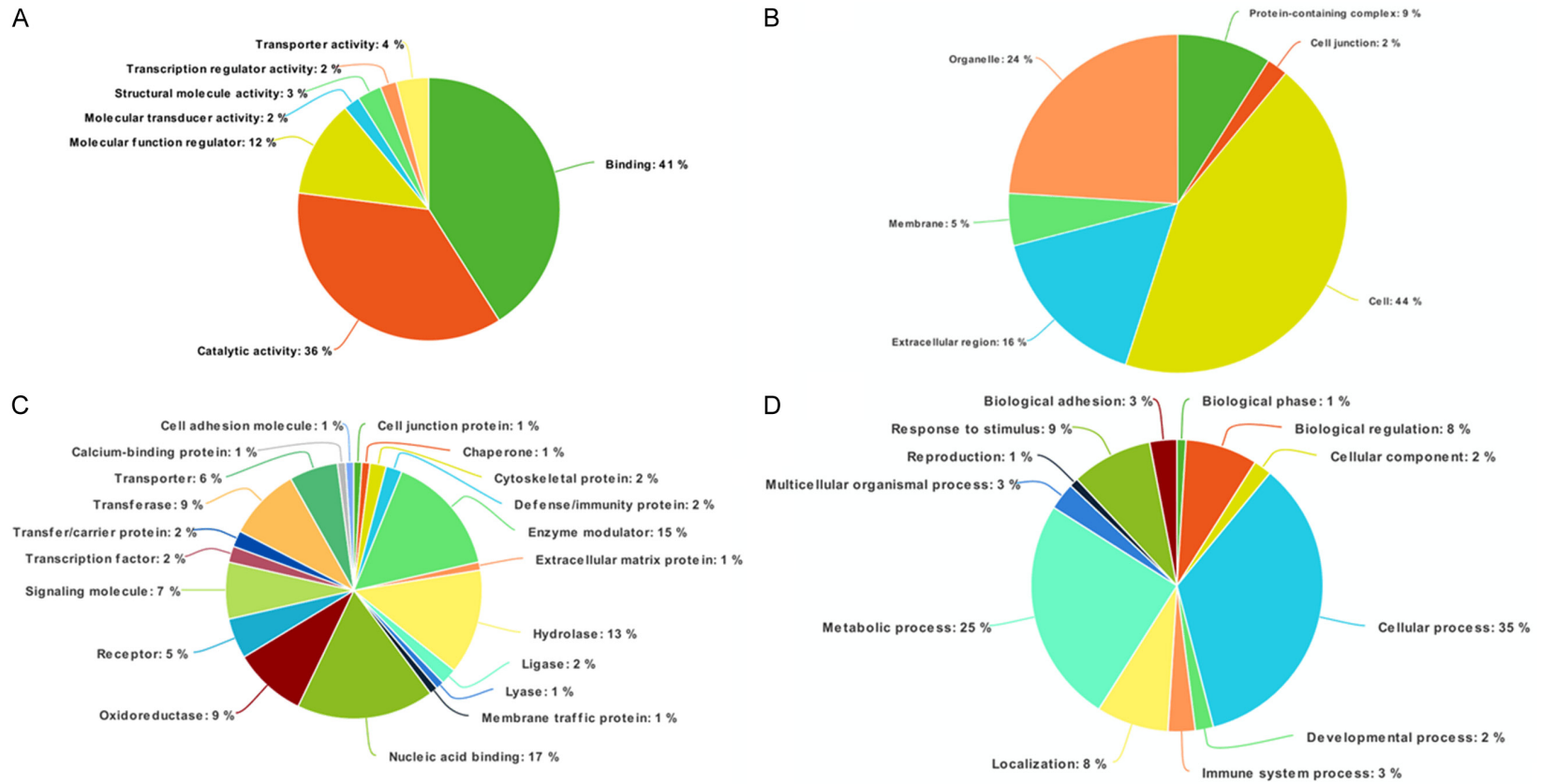


**Figure 5.** Classification of protein function by Panther analysis. The proteins were classified using PANTHER classification system, based on: (A) Molecular function; (B) Biological processes; (C) Cellular components; and (D) Protein class.



## Effectiveness of BMP inhibition on melanoma

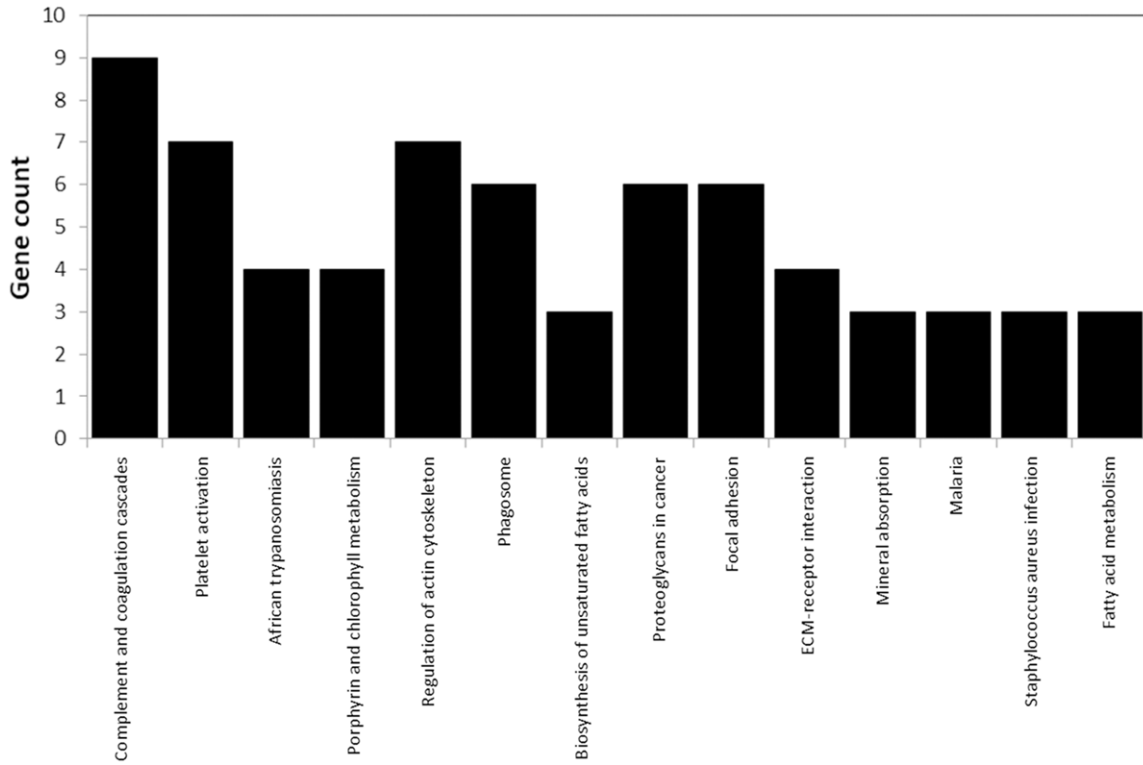


Figure 6. The signaling pathways associated with the proteins identified by DAVID annotation.

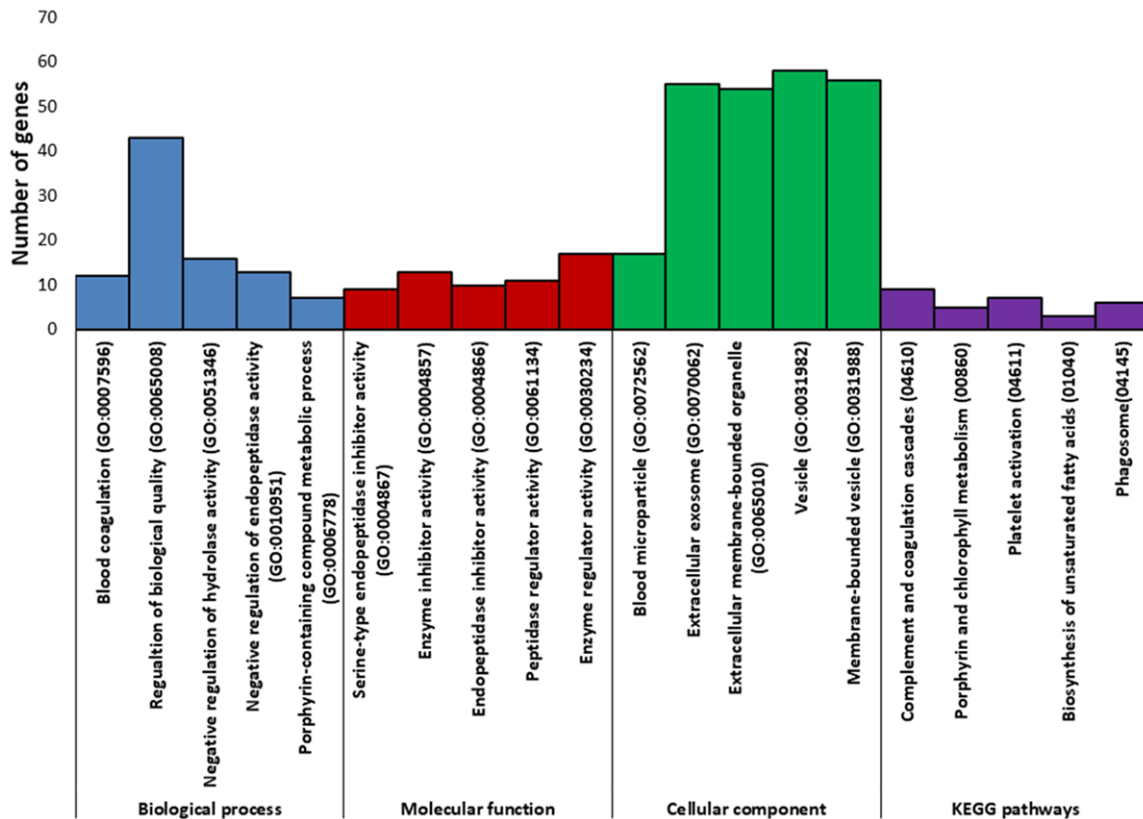
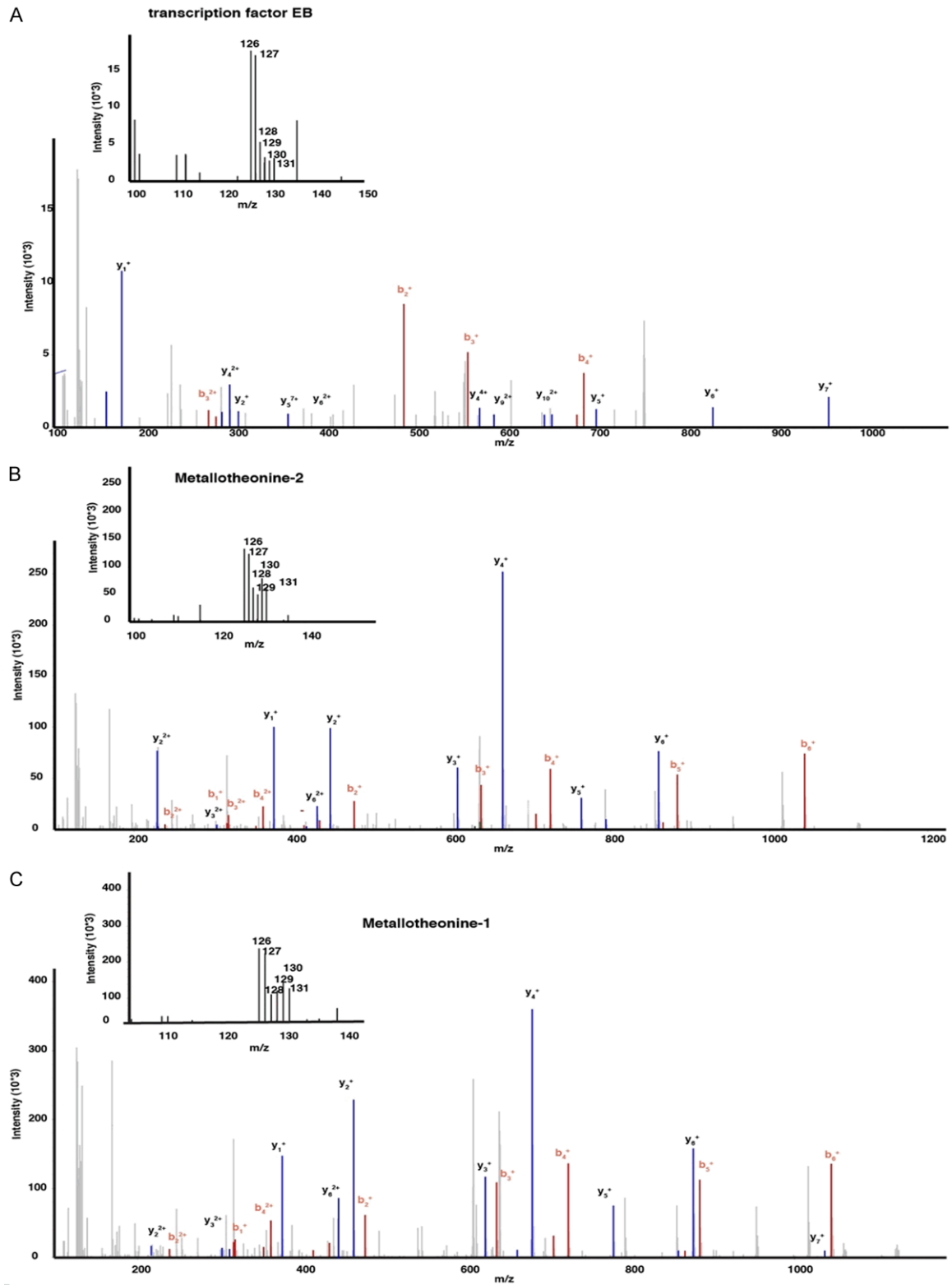


Figure 7. Pathway analysis of the proteins altered in LDN193189 treated melanoma tissue. This analysis was done using the String Protein interaction analysis.

# Effectiveness of BMP inhibition on melanoma



**Figure 8.** Representative MS/MS spectra identified in this study. A. Metallothionein 1; B. Metallothionein 2; C. Transcription factor EB.

Analysis of the melanoma proteome profiles resulted in identifying 117 proteins present at

increased levels while 14 proteins present at reduced levels in mice with melanoma treated

## Effectiveness of BMP inhibition on melanoma

with LDN193189 compared with untreated melanoma.

The most down-regulated proteins included metallothionein (MT) 1 and 2 which are cysteine-rich low molecular mass proteins. The MT is involved in many physiological and pathophysiological processes such as apoptosis, proliferation, angiogenesis, and the detoxification of heavy metals suggesting its role in carcinogenesis and tumor therapy [33]. This study identified the reduced levels of MT1 and MT2 upon inhibition of the BMP pathway in melanoma, suggesting its role in melanoma growth. In the last decade, overexpression of immunohistochemically labeled MTs in paraffin-embedded tissues turned out to be a highly significant prognostic marker in different tumors [34, 35].

The transcription factor EB (TFEB) plays a crucial role in regulating basic cellular processes, such as lysosomal biogenesis and autophagy [36]. TFEB provides a link between the nutrient-sensing mechanistic Target of Rapamycin Complex 1 (mTORC1) machinery and the transcriptional cellular response needed to cope with nutritional stress. Moreover, the interplay of oncogenic KRAS with TFEB and autophagy has been shown to be inversely correlated [37] and have negative impact on Wnt signaling. Therefore, inhibition of BMP pathways may disrupt the RAS signaling with TFEB and induces the cell death of melanoma.

### Conclusion

This study demonstrated the inhibition of the BMP signaling pathway by LDN193189 and showed that it could inhibit tumor growth by regulating the survival of cancer cells. Mass spectrometric analysis showed that inhibition of the BMP signaling cascade with small molecule inhibitors decreased the expression of the MT1 and MT2 which are well known for the anti-apoptotic, antioxidant, proliferative, and angiogenic effects in cancer. Both MT and TFEB proteins are well known regulators of cell death. Ultimately, findings of the present study suggest that inhibition of the BMP pathway may positively affect patients' response to the current chemotherapeutic agents used.

### Acknowledgements

We would also like to acknowledge Yenepoya Research Centre and Department of Bio-

chemistry, Yenepoya (Deemed to be University) for infrastructure and core facility support for conducting this research. The authors also thank the Institute of Bioinformatics, Bangalore for extending the use of HPLC facility and Thermo Fisher Scientific Limited (Mass spectrometry division), Bangalore, for the use of mass spectrometry facility. We also acknowledge the help given by Mr. Saravanan Kumar, Group Leader Proteomics and Biopharma, Proteomics facility, Thermo Fisher Scientific India Pvt Ltd, Bangalore, India. The work was supported by funding from Board of Research in Nuclear Sciences (Ref no. 2013/34/8) sanctioned to DU and Yenepoya University Seed grant (Ref no. YU/YRC/Seed Grant/2016) to VRP. BSK received financial assistance as Senior Research Fellowship (Ref No. 08/652(001)/2017-EMR-I) from Council for Scientific and Industrial Research (CSIR), India.

### Disclosure of conflict of interest

None.

**Address correspondence to:** Dr. Vinitha Ramanath Pai, Department of Biochemistry, Yenepoya Medical College, Yenepoya (Deemed to be University), Mangaluru 575018, Karnataka, India. Tel: +0091-9980145182; E-mail: vinitharpai@gmail.com

### References

- [1] US Department of Health and Human Services. Skin cancer as a major public health problem. The surgeon general's call to action to prevent skin cancer. Washington (DC): 2014.
- [2] American Cancer Society. "Cancer facts and figures 2020". Atlanta: American Cancer Society; 2020.
- [3] Chantharasamee J and Treetipsatit J. Metastatic melanoma of uncertain primary with 5-year durable response after conventional therapy: a case report with literature review. *Case Rep Oncol Med* 2018; 2018: 7289896.
- [4] Kalal BS, Upadhy D and Pai VR. Chemotherapy resistance mechanisms in advanced skin cancer. *Oncol Rev* 2017; 11: 326.
- [5] Krattinger R, Ramelyte E, Dornbierer J and Dummer R. Is single versus combination therapy problematic in the treatment of cutaneous melanoma? *Expert Rev Clin Pharmacol* 2019; 14: 9-23.
- [6] Wong DJ and Ribas A. Targeted therapy for melanoma. *Cancer Treat Res* 2016; 167: 251-262.
- [7] Dratkiewicz E, Simiczjew A, Pietraszek-Gremplewicz K, Mazurkiewicz J and Nowak D. Char-

## Effectiveness of BMP inhibition on melanoma

- acterization of melanoma cell lines resistant to vemurafenib and evaluation of their responsiveness to EGFR- and MET-inhibitor treatment. *Int J Mol Sci* 2019; 21: 113.
- [8] Rothhammer T, Poser I, Soncin F, Bataille F, Moser M and Bosserhoff AK. Bone morphogenetic proteins are overexpressed in malignant melanoma and promote cell invasion and migration. *Cancer Res* 2005; 65: 448-456.
- [9] Hsu MY, Rovinsky S, Penmatcha S, Herlyn M and Muirhead D. Bone morphogenetic proteins in melanoma: angel or devil? *Cancer Metastasis Rev* 2005; 24: 251-263.
- [10] Guo X and Wang XF. Signaling cross-talk between TGF-beta/BMP and other pathways. *Cell Res* 2009; 19: 71-88.
- [11] Bach DH, Park HJ and Lee SK. The dual role of bone morphogenetic proteins in cancer. *Mol Ther Oncolytics* 2017; 8: 1-13.
- [12] Zhang L, Ye Y, Long X, Xiao P, Ren X and Yu J. BMP signaling and its paradoxical effects in tumorigenesis and dissemination. *Oncotarget* 2016; 7: 78206-78218.
- [13] Guicheux J, Lemonnier J, Ghayor C, Suzuki A, Palmer G and Caverzasio J. Activation of p38 mitogen-activated protein kinase and c-Jun-NH2-terminal kinase by BMP-2 and their implication in the stimulation of osteoblastic cell differentiation. *J Bone Miner Res* 2003; 18: 2060-2068.
- [14] Sanvitale CE, Kerr G, Chaikuad A, Ramel MC, Mohedas AH, Reichert S, Wang Y, Triffitt JT, Cuny GD, Yu PB, Hill CS and Bullock AN. A new class of small molecule inhibitor of BMP signaling. *PLoS One* 2013; 8: e62721.
- [15] Vogt J, Traynor R and Sapkota GP. The specificities of small molecule inhibitors of the TGFβs and BMP pathways. *Cell Signal* 2011; 23: 1831-1842.
- [16] van Meerloo J, Kaspers GJ and Cloos J. Cell sensitivity assays: the MTT assay. *Methods Mol Biol* 2011; 731: 237-245.
- [17] Kalal BS, Pai VR, Behera SK and Somashekarappa HM. HDAC2 inhibitor valproic acid increases radiation sensitivity of drug-resistant melanoma cells. *Med Sci (Basel)* 2019; 7: 51.
- [18] Kalal BS, Pai VR and Upadhy D. Valproic acid reduces tumor cell survival and proliferation with inhibitors of downstream molecules of epidermal growth factor receptor pathway. *J Pharmacol Pharmacother* 2018; 9: 11-16.
- [19] Marimuthu A, O'Meally RN, Chaerkady R, Subbannayya Y, Nanjappa V, Kumar P, Kelkar DS, Pinto SM, Sharma R, Renuse S, Goel R, Christopher R, Delanghe B, Cole RN, Harsha HC and Pandey A. A comprehensive map of the human urinary proteome. *J Proteome Res* 2011; 10: 2734-2743.
- [20] Huang DW, Sherman BT, Tan Q, Collins JR, Alvord WG, Roayaei J, Stephens R, Baseler MW, Lane HC and Lempicki RA. The DAVID gene functional classification tool: a novel biological module-centric algorithm to functionally analyze large gene lists. *Genome Biol* 2007; 8: R183.
- [21] Mi H, Huang X, Muruganujan A, Tang H, Mills C, Kang D and Thomas PD. PANTHER version 11: expanded annotation data from gene ontology and reactome pathways, and data analysis tool enhancements. *Nucleic Acids Res* 2017; 45: D183-D189.
- [22] Keshava Prasad TS, Goel R, Kandasamy K, Keerthikumar S, Kumar S, Mathivanan S, Telikicherla D, Raju R, Shafreen B, Venugopal A, Balakrishnan L, Marimuthu A, Banerjee S, Somanathan DS, Sebastian A, Rani S, Ray S, Harrys Kishore CJ, Kanth S, Ahmed M, Kashyap MK, Mohmood R, Ramachandra YL, Krishna V, Rahiman BA, Mohan S, Ranganathan P, Ramabadran S, Chaerkady R and Pandey A. Human protein reference database—2009 update. *Nucleic Acids Res* 2009; 37: D767-772.
- [23] Szklarczyk D, Morris JH, Cook H, Kuhn M, Wyder S, Simonovic M, Santos A, Doncheva NT, Roth A, Bork P, Jensen LJ and von Mering C. The STRING database in 2017: quality-controlled protein-protein association networks, made broadly accessible. *Nucleic Acids Res* 2017; 45: D362-D368.
- [24] Perez-Riverol Y, Csordas A, Bai J, Bernal-Llinares M, Hewapathirana S, Kundu DJ, Inuganti A, Griss J, Mayer G, Eisenacher M, Perez E, Uszkoreit J, Pfeuffer J, Sachsenberg T, Yilmaz S, Tiwary S, Cox J, Audain E, Walzer M, Jarnuczak AF, Ternent T, Brazma A and Vizcaino JA. The PRIDE database and related tools and resources in 2019: improving support for quantification data. *Nucleic Acids Res* 2019; 47: D442-D450.
- [25] Choi S, Yu J, Park A, Dubon MJ, Do J, Kim Y, Nam D, Noh J and Park KS. BMP-4 enhances epithelial mesenchymal transition and cancer stem cell properties of breast cancer cells via notch signaling. *Sci Rep* 2019; 9: 11724.
- [26] Ali JL, Lagasse BJ, Minuk AJ, Love AJ, Moraya AI, Lam L, Arthur G, Gibson SB, Morrison LC, Werbowetski-Ogilvie TE, Fu Y and Nachtigal MW. Differential cellular responses induced by dorsomorphin and LDN-193189 in chemotherapy-sensitive and chemotherapy-resistant human epithelial ovarian cancer cells. *Int J Cancer* 2015; 136: E455-469.
- [27] Vollaire J, Machuca-Gayet I, Lavaud J, Bellanger A, Bouazza L, El Moghrabi S, Treilleux I, Coll JL, Peyruchaud O, Josserand V and Cohen PA. The bone morphogenetic protein signaling inhibitor LDN-193189 enhances metastasis development in mice. *Front Pharmacol* 2019; 10: 667.

## Effectiveness of BMP inhibition on melanoma

- [28] Owens P, Pickup MW, Novitskiy SV, Giltneane JM, Gorska AE, Hopkins CR, Hong CC and Moses HL. Inhibition of BMP signaling suppresses metastasis in mammary cancer. *Oncogene* 2015; 34: 2437-2449.
- [29] Boergermann JH, Kopf J, Yu PB and Knaus P. Dorsomorphin and LDN-193189 inhibit BMP-mediated Smad, p38 and Akt signalling in C2C12 cells. *Int J Biochem Cell Biol* 2010; 42: 1802-1807.
- [30] Yu PB, Deng DY, Lai CS, Hong CC, Cuny GD, Bouxsein ML, Hong DW, McManus PM, Katagiri T, Sachidanandan C, Kamiya N, Fukuda T, Mishina Y, Peterson RT and Bloch KD. BMP type I receptor inhibition reduces heterotopic [corrected] ossification. *Nat Med* 2008; 14: 1363-1369.
- [31] Dinter T, Bocobo GA and Yu PB. Pharmacologic strategies for assaying BMP signaling function. *Methods Mol Biol* 2019; 1891: 221-233.
- [32] Sengupta D and Tackett AJ. Proteomic findings in melanoma. *J Proteomics Bioinform* 2016; 9: e29.
- [33] Bizon A, Jedryczko K and Milnerowicz H. The role of metallothionein in oncogenesis and cancer treatment. *Postepy Hig Med Dosw (Online)* 2017; 71: 98-109.
- [34] Weinlich G. Metallothionein-overexpression as a prognostic marker in melanoma. *G Ital Dermatol Venereol* 2009; 144: 27-38.
- [35] Mangelinck A, da Costa MEM, Stefanovska B, Bawa O, Polrot M, Gaspar N and Fromigue O. MT2A is an early predictive biomarker of response to chemotherapy and a potential therapeutic target in osteosarcoma. *Sci Rep* 2019; 9: 12301.
- [36] Napolitano G and Ballabio A. TFEB at a glance. *J Cell Sci* 2016; 129: 2475-2481.
- [37] Moruno-Manchon JF, Uzor NE, Kesler SR, Wefel JS, Townley DM, Nagaraja AS, Pradeep S, Mangala LS, Sood AK and Tsvetkov AS. TFEB ameliorates the impairment of the autophagy-lysosome pathway in neurons induced by doxorubicin. *Aging (Albany NY)* 2016; 8: 3507-3519.

## Effectiveness of BMP inhibition on melanoma

**Supplementary Table 1.** The complete list of altered proteins identified in LDN193189 treated melanoma

7.81305482766309	<b>Car2</b>	PREDICTED: carbonic anhydrase 2 isoform X1 [Mus musculus]
6.06124047893559	<b>Hbb-bt</b>	hemoglobin, beta adult t chain [Mus musculus]
4.56571440714456	<b>Hba-a2</b>	PREDICTED: parvalbumin alpha isoform X1 [Mus musculus]
4.24275326424469	<b>Slc4a1</b>	hemoglobin alpha, adult chain 2 [Mus musculus]
3.95263578088825	<b>Scrn3</b>	PREDICTED: secernin-3 isoform X1 [Mus musculus]
3.93318186278628	<b>Fga</b>	band 3 anion transport protein [Mus musculus]
3.58299237700525	<b>Fgg</b>	fibrinogen alpha chain isoform 1 preproprotein [Mus musculus]
3.42715246764455	<b>Fgb</b>	fibrinogen gamma chain isoform 2 precursor [Mus musculus]
3.36017529547672	<b>Golt1b</b>	fibrinogen beta chain preproprotein [Mus musculus]
3.15549244182021	<b>Car1</b>	troponin C, skeletal muscle [Mus musculus]
3.03640574092216	<b>Spta1</b>	creatine kinase M-type [Mus musculus]
2.84005173248478	<b>Sptb</b>	thymosin beta-4 [Mus musculus]
2.81677406997486	<b>Dnttip1</b>	myosin regulatory light chain 2, skeletal muscle isoform [Mus musculus]
2.79564585151014	<b>Tubb1</b>	PREDICTED: gamma-enolase isoform X1 [Mus musculus]
2.76151187643348	<b>Bpgm</b>	non-secretory ribonuclease precursor [Mus musculus]
2.65405284423052	<b>Alad</b>	PREDICTED: troponin T, fast skeletal muscle isoform X27 [Mus musculus]
2.61927869199693	<b>Prpf4b</b>	myosin-4 [Mus musculus]
2.5349238662671	<b>Slc14a1</b>	keratin, type II cytoskeletal 79 [Mus musculus]
2.53202478522876	<b>Slc16a1</b>	PREDICTED: myosin light chain 1/3, skeletal muscle isoform isoform X1 [Mus musculus]
2.49592735040191	<b>Ostc</b>	alpha-actinin-3 [Mus musculus]
2.47485467430782	<b>Ect2</b>	PREDICTED: acyl carrier protein, mitochondrial isoform X1 [Mus musculus]
2.4596068288634	<b>Itga2b</b>	carbonic anhydrase 3 [Mus musculus]
2.44405817814349	<b>Ank1</b>	collagen alpha-1(III) chain preproprotein [Mus musculus]
2.39602219845429	<b>LOC100862446</b>	PREDICTED: vesicle transport protein GOT1B isoform X1 [Mus musculus]
2.37804180317328	<b>Aldh1a1</b>	spectrin alpha chain, erythrocytic 1 [Mus musculus]
2.35847285488141	<b>Apcs</b>	carbonic anhydrase 1 [Mus musculus]
2.29161971393249	<b>Ndufab1</b>	PREDICTED: troponin I, fast skeletal muscle isoform X1 [Mus musculus]
2.23788619410039	<b>Fgf1</b>	eosinophil peroxidase precursor [Mus musculus]
2.21915822259405	<b>Hagh</b>	calsequestrin-1 precursor [Mus musculus]
2.14473456862074	<b>Orm2</b>	monocarboxylate transporter 1 [Mus musculus]
2.12192643753893	<b>Vtn</b>	tubulin beta-1 chain [Mus musculus]
2.09986917063155	<b>Aqp1</b>	spectrin beta chain, erythrocytic [Mus musculus]
2.09094170616422	<b>Slc2a3</b>	PREDICTED: beta-enolase isoform X1 [Mus musculus]
2.08889989616192	<b>Hbb-b1</b>	tubulin alpha-1C chain [Mus musculus]
2.08685223181098	<b>Dhx36</b>	deoxynucleotidyltransferase terminal-interacting protein 1 [Mus musculus]
2.08427266201531	<b>Itgb3</b>	uncharacterized protein LOC243944 [Mus musculus]
2.07671205176147	<b>Arl1</b>	PREDICTED: transmembrane protein 132A isoform X1 [Mus musculus]
2.04460885403631	<b>Rfc1</b>	PREDICTED: myosin-binding protein C, fast-type isoform X1 [Mus musculus]
1.98944551920491	<b>Blvrb</b>	serum amyloid P-component precursor [Mus musculus]
1.9818324033103	<b>Orm1</b>	PREDICTED: sarcoplasmic/endoplasmic reticulum calcium ATPase 1 isoform X1 [Mus musculus]
1.98028070769476	<b>Itih4</b>	PREDICTED: serine/threonine-protein kinase PRP4 homolog isoform X1 [Mus musculus]
1.97770488665627	<b>4930433111Rik</b>	protein ECT2 isoform 1 [Mus musculus]
1.94998876063832	<b>2310035C23Rik</b>	triadin [Mus musculus]
1.94724193081876	<b>Dock9</b>	hemoglobin subunit beta-1 [Mus musculus]
1.94690636231881	<b>Epb41</b>	tropomyosin beta chain isoform Tpm2.2st [Mus musculus]
1.94639105063485	<b>Serpina10</b>	bisphosphoglycerate mutase [Mus musculus]
1.93512936923832	<b>Slc45a2</b>	decorin preproprotein [Mus musculus]
1.92523830576195	<b>Fads1</b>	alpha-1-acid glycoprotein 2 precursor [Mus musculus]
1.91893687067975	<b>Ube2l6</b>	tropomyosin alpha-1 chain isoform Tpm1.13 [Mus musculus]
1.89658466131713	<b>Prdx2</b>	alpha-1-acid glycoprotein 1 precursor [Mus musculus]
1.88673340356257	<b>Txndc9</b>	OTU domain-containing protein 4 isoform 1 [Mus musculus]
1.88099259843325	<b>Apoc1</b>	trimeric intracellular cation channel type A [Mus musculus]
1.85696344820999	<b>Myh11</b>	PREDICTED: delta-aminolevulinic acid dehydratase isoform X1 [Mus musculus]
1.85311593682075	<b>Mpp1</b>	calmin isoform a [Mus musculus]

## Effectiveness of BMP inhibition on melanoma

1.83428106869167	<b>Epb42</b>	membrane-associated transporter protein [Mus musculus]
1.81662426569236	<b>Mbl2</b>	PREDICTED: nebulin isoform X22 [Mus musculus]
1.81203698050939	<b>Fn1</b>	collagen alpha-2(V) chain preproprotein [Mus musculus]
1.80675081093241	<b>Serpina3n</b>	PREDICTED: LIM domain-binding protein 3 isoform X2 [Mus musculus]
1.78271167040169	<b>Exosc7</b>	urea transporter 1 isoform a [Mus musculus]
1.77575944216558	<b>Mcmbp</b>	ATP-dependent RNA helicase DHX36 [Mus musculus]
1.77318792116787	<b>Trip11</b>	guanylate-binding protein 1 [Mus musculus]
1.76360890713569	<b>Src</b>	ADP-ribosylation factor-like protein 1 [Mus musculus]
1.74928009746887	<b>Rpf2</b>	PREDICTED: solute carrier family 2, facilitated glucose transporter member 3 isoform X1 [Mus musculus]
1.74108650104836	<b>Hmbs</b>	macrophage mannose receptor 1 precursor [Mus musculus]
1.71524157691522	<b>Serpina3m</b>	vitronectin precursor [Mus musculus]
1.71203226188581	<b>Ift20</b>	pleckstrin homology domain-containing family O member 2 [Mus musculus]
1.71117309882143	<b>Bcat2</b>	PREDICTED: fibroblast growth factor 1 isoform X1 [Mus musculus]
1.71079727944208	<b>Hpx</b>	PREDICTED: replication factor C subunit 1 isoform X1 [Mus musculus]
1.70903222637221	<b>Isg15</b>	protein MANBAL [Mus musculus]
1.70741261306143	<b>C3</b>	hydroxyacylglutathione hydrolase, mitochondrial isoform 1 precursor [Mus musculus]
1.70735261431771	<b>Rab3d</b>	PREDICTED: ankyrin-1 isoform X1 [Mus musculus]
1.70577785711834	<b>Isoc2a</b>	PREDICTED: ferritin light chain 1 [Mus musculus]
1.69383910305866	<b>Psmc6</b>	PREDICTED: myomesin-2 isoform X1 [Mus musculus]
1.68533985059487	<b>Abcc10</b>	syntaxin-5 [Mus musculus]
1.66541926615576	<b>Cpb2</b>	oligosaccharyltransferase complex subunit OSTC [Mus musculus]
1.65409604102772	<b>Tmtc3</b>	PREDICTED: Golli-Mbp isoform X1 [Mus musculus]
1.6524798655299	<b>Tuba1c</b>	myomesin-1 isoform 1 [Mus musculus]
1.64517612150469	<b>Cyp4f16</b>	60S ribosomal protein L22-like 1 [Mus musculus]
1.64514809083809	<b>Tmem132a</b>	PREDICTED: myosin-6 isoform X1 [Mus musculus]
1.64495987438423	<b>Krt79</b>	PREDICTED: branched-chain-amino-acid aminotransferase, mitochondrial isoform X1 [Mus musculus]
1.63793501525199	<b>Plscr1</b>	adenylate kinase isoenzyme 1 isoform 1 [Mus musculus]
1.62542498919982	<b>Ndc1</b>	integrin alpha-IIb precursor [Mus musculus]
1.62055316050834	<b>Vwa8</b>	60S ribosomal protein L35a [Mus musculus]
1.61806184247657	<b>Pzp</b>	keratin, type II cytoskeletal 5 [Mus musculus]
1.6164903680189	<b>Sart3</b>	retinal dehydrogenase 1 [Mus musculus]
1.60244752487675	<b>Stra13</b>	PREDICTED: neuronal proto-oncogene tyrosine-protein kinase Src isoform X1 [Mus musculus]
1.60115550986864	<b>Pip4k2a</b>	mannose-binding protein C precursor [Mus musculus]
1.59477620425023	<b>Lrg1</b>	interleukin-1 receptor accessory protein isoform d precursor [Mus musculus]
1.59377053226796	<b>Acox1</b>	glycogen phosphorylase, muscle form [Mus musculus]
1.59359630629501	<b>Orc4</b>	aquaporin-1 [Mus musculus]
1.58760119591581	<b>Otud4</b>	PREDICTED: UBX domain-containing protein 4 isoform X1 [Mus musculus]
1.58304318949922	<b>Rpl35a</b>	PDZ and LIM domain protein 7 isoform a [Mus musculus]
1.57468510015356	<b>Stx5a</b>	PREDICTED: titin isoform X1 [Mus musculus]
1.57417005813389	<b>Camk1</b>	PREDICTED: thioredoxin domain-containing protein 9 isoform X1 [Mus musculus]
1.57193790845699	<b>Noc4l</b>	PREDICTED: protein 4.1 isoform X12 [Mus musculus]
1.56833469118492	<b>Mrc1</b>	flavin reductase (NADPH) isoform 1 [Mus musculus]
1.56695057608567	<b>Aldh8a1</b>	fatty acid desaturase 1 [Mus musculus]
1.56299583599738	<b>Il1rap</b>	PREDICTED: keratin, type I cytoskeletal 10 isoform X1 [Mus musculus]
1.55861838556696	<b>Pklr</b>	integrin beta-3 precursor [Mus musculus]
1.54927688527601	<b>Apoc3</b>	isochorismatase domain-containing protein 2A precursor [Mus musculus]
1.54141089097304	<b>Stk24</b>	UDP-glucuronosyltransferase 1-1 precursor [Mus musculus]
1.54023167496475	<b>Hmgcs1</b>	PREDICTED: transmembrane and TPR repeat-containing protein 3 isoform X1 [Mus musculus]
1.54018214293489	<b>Enpp4</b>	sodium channel subunit beta-2 precursor [Mus musculus]
1.53504687297477	<b>F10</b>	PREDICTED: liH domain and HEAT repeat-containing protein KIAA1468 isoform X1 [Mus musculus]
1.52947669951357	<b>Cox7a2</b>	xanthine dehydrogenase/oxidase [Mus musculus]
1.52502889768214	<b>Serpinc1</b>	PREDICTED: fibrillin-1 isoform X1 [Mus musculus]
1.52488349886559	<b>Ppp1ca</b>	cytochrome c oxidase subunit 7A2, mitochondrial precursor [Mus musculus]
1.52416889688743	<b>Urod</b>	protein Z-dependent protease inhibitor isoform 1 precursor [Mus musculus]
1.52338650774788	<b>Itih3</b>	RNA-binding protein PNO1 [Mus musculus]
1.52332120235198	<b>Cat</b>	PREDICTED: 5-oxoprolinase isoform X1 [Mus musculus]
1.52014117931161	<b>Clu</b>	PREDICTED: ras GTPase-activating protein-binding protein 2 isoform X1 [Mus musculus]

## Effectiveness of BMP inhibition on melanoma

1.51997269916242	Gclm	PREDICTED: metal-response element-binding transcription factor 2 isoform X1 [Mus musculus]
1.51276287772238	Apoa1	PREDICTED: sphingomyelin phosphodiesterase 4 isoform X1 [Mus musculus]
1.50971038308367	Sf1	inter alpha-trypsin inhibitor, heavy chain 4 isoform 1 precursor [Mus musculus]
1.50969855447155	Hpn	PREDICTED: ras-related protein Rab-3D isoform X1 [Mus musculus]
1.50618288043433	Tmx3	protein S100-A1 [Mus musculus]
1.50098888986133	Fam213a	cathepsin S isoform 1 preproprotein [Mus musculus]
0.594325043716454	Tfeb	PREDICTED: transmembrane emp24 domain-containing protein 2 [Mus musculus]
0.583816277324409	Gbp6	alpha-1-antitrypsin 1-1 isoform 2 [Mus musculus]
0.582439745206939	Otud6b	proteasome assembly chaperone 1 [Mus musculus]
0.558059366397443	Serpina3c	inward rectifier potassium channel 13 [Mus musculus]
0.537792984111883	Hmgcn2	serine protease inhibitor A3K precursor [Mus musculus]
0.527877109831677	Hmga1	heat shock protein beta-1 [Mus musculus]
0.485492101444739	Hspb1	haptoglobin precursor [Mus musculus]
0.477186279715409	Hacd2	histone H2A type 2-A [Mus musculus]
0.361496834078707	Hist2h2aa2	alpha-1-antitrypsin 1-5 precursor [Mus musculus]
0.355364907938917	Serpina1e	transcription factor EB isoform a [Mus musculus]
0.334715833423526	Hmga1	PREDICTED: YY1-associated factor 2 isoform X1 [Mus musculus]
0.286079020941757	Mt1	metallothionein-1 [Mus musculus]
0.276098550548476	Ccdc126	coiled-coil domain-containing protein 126 isoform 1 precursor [Mus musculus]
0.266850130279332	Mt2	metallothionein-2 [Mus musculus]

The data obtained for LC-MS/MS was analyzed using Proteome discoverer 2.1, which compares the LC-MS/MS data against mouse database. This table shows the altered proteins with a relative abundance of more than 1.5 times (red color) and lower than 0.6 times (green color) with their gene symbol, and full form as compared in LDN193189 treated v/s untreated melanoma tumor.